Removal of chlorinated volatile organic compounds onto natural and Cu-modified zeolite: The role of chemical surface characteristics in the adsorption mechanism

Héctor Valdés, Andrés L Riquelme, Víctor A Solar, Federico Azzolina-Jury, Frederic Thibault-Starzyk

Removal of chlorinated volatile organic compounds onto natural and Cu-modified zeolite: The role of chemical surface characteristics in the adsorption mechanism

Héctor Valdés [1*], Andrés L. Riquelme [1], Víctor A. Solar [1], Federico Azzolina-Jury [2], Frédéric Thibault-Starzyk [3]

[1] Clean Technologies Laboratory (F. Ingeniería). Universidad Católica de la Santísima Concepción, Alonso de Ribera 2850, Concepción, Chile

[2] Normandie Université, ENSICAEN, UNICAEN, CNRS, Laboratoire Catalyse et Spectrochimie, 14000, Caen, France

[3] Maison Française d'Oxford, CNRS, MEAE, 2-10 Norham Rd, Oxford OX2 6SE, United Kingdom

*Corresponding author. Tel.: +56-41-2345044; fax: +56-41-2345300;

E-mail address: hvaldes@ucsc.cl (H. Valdés)

Abstract

In this study, the effect of chemical surface characteristics of natural and Cu-modified zeolite in the adsorption of chlorinated volatile organic compounds (VOC_{Cls}) was investigated using infrared spectroscopy. A natural zeolite mainly comprised of clinoptilolite and mordenite was used as a parent material. A succession of chemical and thermal treatments produced a Cu-modified natural zeolite (NZ-Cu) with higher adsorption properties toward the elimination of VOC_{Cls}. The adsorption of VOC_{Cls} onto NZ-Cu zeolite could be explained by a surface mechanism that comprises the interaction not only with Brønsted acid sites present on the original natural zeolite framework; but also with new Brønsted acid sites formed after the successive treatments.

Keywords: Adsorption mechanism, Brønsted acid sites; chlorobenzene; infrared spectroscopy, natural zeolite; perchloroethylene.

1. Introduction

Chlorinated volatile organic compounds (VOC_{Cls}) are one of the major sources of air and water pollution [1,2]. VOC_{Cls} play an important role in the chemical and pharmaceutical industries, where they are used as solvents and reagents. They are employed in aerosols, adhesives and in degreasers in many industrial manufacturing processes as well as in the dry cleaning industry [1,3]. About 1.5 million tons of chlorinated compounds are released into the atmosphere each year [4]. Most of these compounds are man-made and are known to be irritants, toxics, carcinogens, and flammables [5]. VOC_{Cls} are mainly regarded as xenobiotics, resistant to biodegradation and therefore they are very persistent in the environment [6]. Among VOC_{Cls}, carbon tetrachloride, trichloroethane, trichlorethylene and trichlorotoluene can cause significant damage to the environment [7]. Emissions of these compounds into the atmosphere contribute to the destruction of the ozone layer, to the formation of photochemical smog and global warming. In many countries, the concern about the emissions of VOC_{Cls} has increased in the last years; which has led to the emergence of stronger and more restrictive environmental regulations [3,8].

There are some available emission control techniques for the elimination of VOC_{Cls}; each one has its own advantages and limitations. Among more conventional treatment processes to control the emissions of VOC_{Cls}; adsorption, thermal oxidation, wet scrubbing, catalytic oxidation and biofiltration are included [4,9-11]. Adsorption has been widely used as a reliable alternative process to abate VOC_{Cls} from industrial emissions due to flexibility, low energy consumption and cheap operating costs [3,12,13]. Microporous materials such as activated carbons, synthetic and natural zeolites have been used as adsorbents in the elimination of VOC_{Cls}, since their microporosity acts as a gaseous reservoir [14].

Activated carbons are commonly selected as adsorbents in many industrial cases due to their high adsorption capacities. However, activated carbons are relatively expensive and

difficult to regenerate due to their sensibility to high temperatures and the possibility to ignite [9,15]. On the other hand, synthetic and natural zeolites have been used as adsorbents in the removal of VOC_{Cls} from waste gas streams [12,16-18], being attractive alternatives from the technical and economic point of view [14]. Zeolites have a high thermal stability [19], which makes them easy to regenerate and to reuse for further process cycles [20,21]. Unfortunately, the low adsorption capacities of natural zeolites toward VOC_{Cls} make them uncompetitive in comparison to activated carbons. Such limitation can be overcome by chemically modifying natural zeolites in order to increase their adsorption capacities. Recent results show an increase in the removal of VOCs using modified natural zeolite with low cost transition metals such as Co, Cu, Mn, and Fe [22-25]. A surface response methodology based on a D-Optimal design of experiments has been applied to identify the transition metal-modified natural zeolite with the highest adsorption capacity for VOC_{Cls} [26]. A succession of ion-exchange with ammonium (0.1 mol dm^{-3}), thermal out-gassing (350°C), and ion-exchange (0.05 mol Cu^{2+} dm^{-3}), followed by calcination and reduction at 350°C, is claimed to produce a modified natural zeolite with optimal adsorption properties for the elimination of VOC_{Cls} [26].

Unfortunately, there is a lack of information on the influence of chemical surface characteristics of natural and Cu-modified zeolite on the adsorption of VOC_{Cls}. This work aims at some of these issues. In this study, the nature and strength of acidic surface sites of natural and Cu-modified zeolite are characterised by infrared Fourier transform spectroscopy (FTIR) using pyridine and deuterated acetonitrile as probe molecules. Two different VOC_{Cls} (perchlorethylene and chlorobenzene) are used here in order to evaluate the effect of the chemical properties of the adsorbate on the adsorption mechanism. In addition, diffuse reflectance infrared Fourier transform spectroscopy (DRIFTS) is applied to study the adsorption of VOC_{Cls} on natural and Cu-modified zeolites. Surface active centres are

identified and the nature of their interaction with VOC_{Cls} are characterised at a molecular level. Moreover, temperature-programmed desorption (TPD) experiments are conducted in order to obtain information about the adsorption energetic of the VOC_{Cls}/zeolite interactions. Finally, a surface mechanism is proposed for the adsorption of VOC_{Cls} over natural and Cu-modified zeolites.

2. Experimental

2.1. Materials

Natural zeolite (NZ) was supplied by the Chilean mining company "*Minera Formas*". NZ was ground and sieved to 0.300–0.425 mm; then it was rinsed with ultra pure water, oven-dried at 125°C for 24 h, and stored in a desiccator until its further use. This zeolite is composed of clinoptilolite (53%), mordenite (40%), and quartz (7%) and has been previously characterised using standard techniques, as indicated elsewhere [27]. Table 1 summarises the main physical-chemical properties of this zeolite sample.

Perchlorethylene (PERC) and chlorobenzene (CLB) were supplied by MERCK (Darmstadt, Germany) with a purity > 99% and were used without further purification. The inlet concentration of the target VOC_{Cl} was fixed by vaporising the liquid phase of the VOC_{Cl} in a thermally controlled saturator chamber by bubbling argon and then was diluted by mixing with another fresh stream of argon, until reaching the desired inlet concentration, as described in a previous publication [28]. Gas flow rates were controlled by mass flow controllers provided by Aalborg Instruments & Controls, Inc. (New York, NY, USA).

All gases used in this study were supplied by PRAXAIR Chile Ltda (Concepción, Chile). Argon 99.999% purity was used as a carrier gas, containing O_2 (<1 ppm), N_2 (<3 ppm), H_2O (<2 ppm), CO_2 (<1 ppm) and CO (<1 ppm). Oxygen with 99.8% purity, containing H_2O (<3

ppm), THC (<0.5 ppm) was used in the calcination treatment. Hydrogen at 5% (v/v) in argon was applied in the zeolite post-treatment.

Cu was used here as an active transition metal for natural zeolite modification. It was supplied in the form of metal salt by MERCK (Darmstadt, Germany) as copper nitrate ($Cu(NO_3)_2 \cdot 3H_2O$) with a purity > 99%. Water used in chemical modification treatments was ultra-pure water (≥18.0 MΩ cm) and was obtained from an EASY pure® RF II system (Barnstead|Thermolyne Corp., Dubuque, IA, USA).

2.2. Modification treatment of natural zeolite

The natural zeolite (NZ) was chemically and thermally modified by a succession of two ion-exchange pre-treatments using ammonium salt, followed by thermal out-gassing at 350°C; where Cu^{2+} ions were brought into the natural modified zeolite by ion-exchange, followed by calcination in O_2 flow at 350°C and reduction in H_2 flow at 350°C. A more detailed description of each modification step is given below:

Firstly, NZ was modified by two successive ion-exchange treatments using an ammonium sulphate solution (0.1 mol dm^{-3}) in order to remove any unwanted cation and prepare the purely acidic form of the zeolite. A ratio of 1.0 g of NZ per 10 cm^3 of solution was applied. Then, the mix was shaken for 2 h at 90°C and 27 rpm in a thermo-regulated bath (LSB-015S model, Korea). After that, the sample was rinsed with ultra-pure water at 90°C and 27 rpm for 2 h. Ultra-pure water was renovated two times, each one after 1 hour of washing to eliminate the excess of salt. Subsequently, a second ion-exchange using the ammonium sulphate solution was conducted, following the same steps and experimental conditions as described before. Finally, ammonium-exchanged zeolite sample was dried at 125°C for 24 h.

Secondly, the purely acidic form of the zeolite was obtained by thermally out-gassing the ammonium-exchanged zeolite sample in a vertical tubular furnace at 350°C. The sample was

placed in a quartz U-shaped fixed-bed flow contactor (4 mm ID) and heated at a rate of 1°C min^{-1}, under argon flow (100 cm^3 min^{-1}). When the sample reached a temperature of 350°C, isothermal conditions were kept for 2 h, before quenching to room temperature. The succession of two ion-exchanges using ammonium salt followed by a thermal out-gassing at 350°C were applied since, as it is reported elsewhere [27,29,30], these modification pre-treatment steps decrease the content of compensating cations with an increase in the content of Brønsted acidic sites and without a significant change in the Si/Al ratio. A lower content of compensating cations improve the diffusion of target VOCs inside the zeolite framework [27,29,30]. Moreover, experimental evidences have proved that a reduction in the amount of compensating cations united to the generation of new Brønsted acid sites after thermal out-gassing at 350°C plays a fundamental role increasing surface interactions among VOCs and Brønsted active sites [27,29,30].

After that, the sample under acidic form was ion-exchanged in a thermo-regulated bath (LSB-015S model, Korea) using a solution of copper nitrate (0.05 mol dm^{-3}). Ion-exchange took place using a ratio of 1.0 g of the out-gassed sample per 10 cm^3 of copper nitrate solution, under constant shaking (27 rpm) at 90°C for 2 hours. Later, the Cu-exchanged zeolite sample was rinsed using ultra-pure water, applying the same washing procedure as described before and oven-dried at 125°C for 24 h. Subsequently, two sequence post-treatments were applied to the Cu-exchanged zeolite sample. Post-treatments were performed in a vertical tubular furnace. The Cu-exchanged zeolite sample was loaded into the quartz U-shaped fixed-bed flow contactor and calcined under oxygen flow (100 cm^3 min^{-1}), heated at 1°C min^{-1} and isothermal conditions were kept for 4 h at 350°C. After that, the sample was cooled down to 100°C under the same oxygen flow. Then, the sample was let down to room temperature in the absence of any flow. The calcined sample was further subjected to a reduction post-treatment using H_2 at 5% (v/v) in argon flow (20 cm^3 min^{-1}) with a heating rate

of 1°C min^{-1}, up to 350°C. After that, the reduced sample was cooled down to 100°C under the same H_2 /argon flow. Then, the H_2 /argon flow was cut and the sample was cooled to room temperature. It has been demonstrated that the incorporation of copper cations into the zeolite structure improves the adsorption capacity toward VOCs due to the increase of cationic adsorption centres and their interactions with π-electrons of the target VOC molecules [26,27]. Thus, the Cu-modified natural zeolite sample (NZ-Cu) was ready to contact the target VOC_{Cl}.

2.3. Physical–chemical characterisation of natural and Cu-modified zeolite samples

The crystallinities of natural zeolite (NZ) and Cu-modified zeolite (NZ-Cu) samples were verified using a PANalyticalX'Pert PRO diffractometer equipped with CuKα radiation (λ = 0.15418 nm, 40 mA, 45 kV). Diffraction data were collected between 2Θ values of 5° and 50° at intervals of 0.1° and speed of 2° per min.

Specific surface area and pore volume of natural and Cu-modified zeolite samples were determined by nitrogen adsorption-desorption measurements at -196°C using the Brunauer-Emmet-Teller (BET) method and the Barret-Joyner-Halenda (BJH) method in a Micrometrics sorptometer Tri Star 3000. Before nitrogen adsorption, zeolite samples were out-gassed at 350 C for 2 hours.

Fourier transform infrared spectroscopy (FTIR) was used to identify active surface sites of natural and Cu-modified zeolite samples. Zeolite samples were ground using an agate mortar; the resulting powders were pressed (10^7 Pa) into self-supported wafers (2 cm^2 area, 10-20 mg). Then, a wafer was placed into a home-made low temperature quartz cell equipped with KBr windows. A quartz sample holder was used to expose the wafer to the IR beam and to displace it inside a furnace located at the top of the cell for thermal treatments. The IR cell was connected to a vacuum line for evacuation and activation steps ($P_{residual}$ 10^{-3} - 10^{-4} Pa). A

Nicolet Magna 750 IR spectrometer equipped with an MCT detector was used for the acquisition of spectra between 4000 cm^{-1} and 400 cm^{-1}. Natural and Cu-modified zeolite samples were activated at 350°C for 6 h under secondary vacuum. The heating rate was set to 0.5°C min^{-1} in order to avoid any structure damage. Infrared spectra were recorded before (a) and after (b) activation of zeolite samples. Then, samples were cooled down to 150°C under secondary vacuum. After that, pyridine was introduced into the infrared cell system using a calibrated volume of 1.56 cm^3 (6-8 mbar) in order to determine Brønsted and Lewis acidities. IR spectra were recorded at 150°C during the pyridine dosing process.

Quantification of pyridine was also done in the desorption mode: it was introduced into the IR cell (2 Torr at equilibrium pressure) at 200°C for 30 min to ensure good diffusion inside zeolite channels. Afterwards, secondary vacuum was applied during 15 min at the same temperature in order to eliminate physisorbed pyridine over zeolites. Spectra were then recorded at different temperatures from 200°C to 350°C. IR bands at 1545 and 1454 cm^{-1} were integrated. In order to quantify Brønsted and Lewis acidic sites, molar absorption coefficients $\varepsilon_{1545\ cm\text{-}1}$ = 1.8 $cm.\mu mol^{-1}$ and $\varepsilon_{1454\ cm\text{-}1}$ = 1.5 $cm.\mu mol^{-1}$ of the bands at 1545 and 1454 cm^{-1} for Brønsted and Lewis acidic sites were used, respectively [31]. The accessible amount of OH groups was estimated by comparing the IR band areas at 3612 cm^{-1} between the activated samples (without pyridine) and those having pyridine adsorbed on their surface (2 Torr at equilibrium pressure) at 200°C.

Finally, the accessibility of OH groups in small pores and even within the side pockets of the mordenite part of natural and Cu-modified natural zeolite samples was quantified using deuterated acetonitrile (CD_3CN) by comparing the IR band areas at 3612 cm^{-1} between the unloaded samples (without deuterated acetonitrile) and those having CD_3CN adsorbed on their surface (2 Torr at equilibrium pressure) at 200°C. Deuterated acetonitrile (CD_3CN) is

preferred over acetonitrile (CH_3CN) in order to avoid Fermi resonance between the vibration ν(CN) and the combination δ(CH_3) + ν(CC) frequencies [32].

2.4. Adsorption experimental procedures

VOC_{Cl}s adsorption experiments were conducted under dynamic conditions in a quartz U-shaped fixed-bed flow adsorber (4 mm ID) that was connected to a gas chromatograph (GC) coupled with a flame ionisation detector (FID) (Clarus 500 GC, Shelton, CT, USA), as reported elsewhere [28]. Argon was used as a carrier gas containing the target VOC_{Cl} and circulated over the adsorber already loaded with the selected zeolite sample (NZ or NZ-Cu). The outlet concentration of VOC_{Cl}, $C_{VOC_{Cl_t}}$ (μmol cm^{-3}), was recorded continuously by gas chromatography at the adsorber outlet as a function of time, until the zeolite sample reached the VOC_{Cl} saturation. More detailed information about the analytical method used for VOC_{Cl} detection and quantification can be found in a previous publication [28]. The total amount of VOC_{Cl} dynamically adsorbed, q (μmol g^{-1}), was obtained from the breakthrough curve, as follows:

$$q = \frac{F\, C_{VOC_{Cl_{in}}}}{m} \int_0^{t_s} \left(1 - \frac{C_{VOC_{Cl_t}}}{C_{VOC_{Cl_{in}}}} \right) dt \qquad (1)$$

where m is the zeolite mass (g), F is the volumetric flow rate (cm^3 min^{-1}), t_s is the time needed to reach the zeolite saturation with VOC_{Cl} (min), and $C_{VOC_{Cl_{in}}}$ and $C_{VOC_{Cl_t}}$ are the concentration of the target VOC_{Cl} (μmol cm^{-3}) at the adsorber inlet and outlet streams as a function of time, respectively.

2.5. DRIFTS study of surface interactions among zeolite samples and target VOC_{Cl}

Diffuse reflectance infrared Fourier transform spectroscopy (DRIFTS) was applied here to allow distinguishing the various chemical interactions between surface sites on the zeolites

and the target VOC_{Cl}. DRIFTS *operando* experiments were performed using a commercial PIKE DiffusIR™ cell (PIKE Technologies, Fitchburg, WI, USA), containing two ZnSe windows (32 × 3 mm) and a gas flow system that was installed in a Nicolet™ iS™50 spectrometer (Thermo Fisher Scientific Inc., Waltham, MA, USA) equipped with a DTGS detector, as described in a previous publication [28]. A powder sample of natural (or pre-treated) zeolite was loaded into a ceramic cup with a porous base. After that, the loaded cup was placed into the DiffuIR™ chamber. A mirror signal was used here as a reference. Before the measurement, the sample was post-treated inside the DiffuIR™ chamber, following the same calcination and reduction procedures at 350°C as in Section 2.2. Then, a spectrum of the adsorbate free sample was measured. Spectra were collected with 60 scans at a resolution of 4 cm^{-1} over the range of 4000–1100 cm^{-1}. In DRIFTS *operando* experiments, the adsorption of the target VOC_{Cl} (perchloroethylene and chlorobenzene) was conducted using an inlet concentration of 7.6 μmol dm^{-3} at 20°C. The inlet concentration was fixed by vaporising the target VOC_{Cl} in a thermally controlled saturator chamber, as described in Section 2.1. The argon stream containing the target VOC_{Cl} was passed through the DiffuIR™ chamber until reaching the saturation and spectra were registered as a function of time. PIKE TempPro™ software was used for temperature control and data collection. Results were processed with OMNIC 9.0 software.

2.6. Temperature-programmed desorption (TPD) of the adsorbed VOC_{Cl}

VOC_{Cl} TPD experiments were conducted in a temperature-programmable flow micro-contactor loaded with 0.3 g of zeolite sample (NZ or NZ-Cu) and coupled to a GC–FID for VOC_{Cl} detection. Firstly, the target VOC_{Cl} (perchloroethylene or chlorobenzene) was injected (50 cm^3 min^{-1}, 7.6 μmol dm^{-3}) over the zeolite sample (NZ or NZ-Cu) until saturation was reached at 20°C and the excess of VOC_{Cl} was flushed out using argon (50 cm^3 min^{-1}) at the

same temperature. The VOC_{Cl} was then progressively desorbed using a TPD procedure, as described elsewhere [28]. The saturated-sample was heated up to 550°C at a heating rate of 3°C min^{-1} under an argon flow (100 cm^3 min^{-1}). A TPD profile of the evolved VOC_{Cl} was obtained using GC–FID analysis, as described in a previous publication [28]. A concentration profile of the evolution of the desorbed VOC_{Cl} was recorded as a function of temperature. The total amount of desorbed VOC_{Cl} (perchloroethylene or chlorobenzene) per mass of zeolite was determined by integrating the area under the TPD concentration curve, using OriginPro 8 SR0 v8.0725 (B725) software.

3. Results and Discussion

3.1. Physical–chemical characterisation of natural and Cu-modified zeolite samples

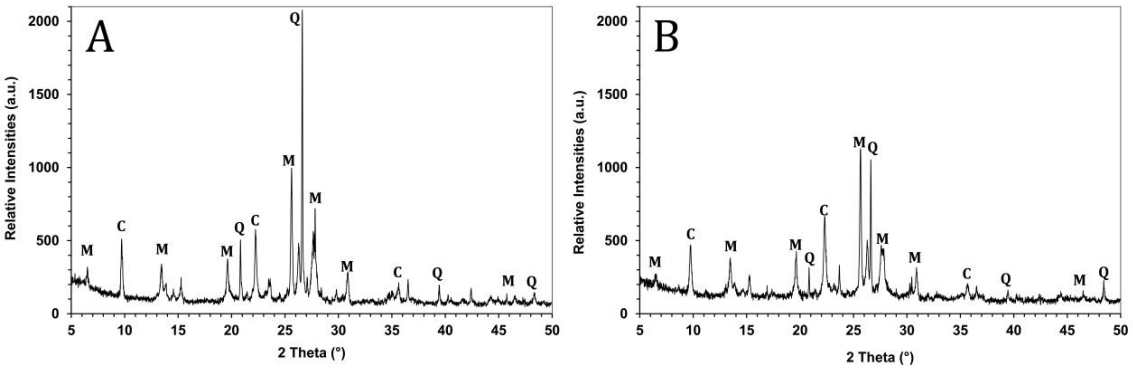

Fig. 1. X-ray powder diffraction patterns: (A) natural zeolite, NZ, (B) Cu-modified natural zeolite, NZ-Cu. (C) Clinoptilolite, (M) Mordenite, (Q) Quartz.

XRD results, shown in Fig. 1-A and 1-B, indicate that no significant changes in the crystalline pattern of natural zeolite are observed after Cu^{2+} ions incorporation and physicochemical treatments. Characteristic peaks of clinoptilolite (C), mordenite (M) and quartz (Q) structures can be observed in the X-ray patterns, according to JCPDS 39-183, JCPDS 29-1257 and JCPDS 461045, respectively. However, a reduction in the intensity of

characteristic peaks of the natural zeolite diffraction pattern after after Cu^{2+} ions incorporation was observed.

Physical characteristics of NZ and NZ-Cu are summarised in Table 1. Results show that specific surface area and pore volume increase after the sequences of physicochemical treatments applied here. Such increases in the values of surface area and pore volume could be related to unblocking porous structure of NZ. It has been reported in previous publication that a combination of ion-exchange treatment using ammonium sulphate followed by thermal out-gassing at 350°C reduces the amount of compensating cations in natural zeolite without significant change on the zeolite framework [33]. The presence of different kinds of compensating cations inside of zeolite framework has been responsible to pore clogging [33]. On the other hand, the observed increase on water adsorption capacity on NZ-Cu could be not only related to physical adsorption of water, but also to water interaction with new Lewis acid surface sites formed after Cu^{2+} ions inclusion inside the zeolite framework. This could, in turn, generate new (weak) Brønsted acid sites.

Table 1. Physical characterisation of natural (NZ) and Cu-modified zeolite (NZ-Cu).

Properties		**NZ**	**NZ-Cu**
Surface area [a] (m^2 g^{-1})	**BET**	241	312
	t-Plot Micropore	224	284
	t-Plot External	17.8	28.8
Pore volume [a] (cm^3 g^{-1})	**Micropore**	0.07	0.11
	Mesopore	0.05	0.06
	Total	0.12	0.17
Average pore diameter [a] (nm)	**BET**	2.2	2.2
	BJH	10.5	8.6
	D-H	9.9	8.3
Water adsorption capacity (%wt-dry)		11.8	13.1

	Si/Al	5.32	5.17
	Si	65.39	67.67
	Al	12.29	13.08
	Ca	11.13	4.12
	Fe	5.27	4.72
	Na	2.12	0.30
	K	1.90	0.88
Elemental analysis [b] (%)	**Ti**	0.89	0.74
	Mg	0.53	0.24
	Mn	0.13	0.08
	Sr	0.12	0.08
	S	0.05	0.05
	Zr	0.05	0.04
	Zn	0.02	0.02
	Cu	ND	7.88

[a] Determined from nitrogen adsorption-desorption isotherms

[b] Determined by X-Ray Fluorescence

Fig. 2-A and 2-B display IR spectra recorded before (a) and after (b) activation of NZ and NZ-Cu, respectively. The IR band at 1630 cm^{-1} is assigned to the bending vibration of OH groups of surface water molecules adsorbed on zeolites [34]. This band is suppressed after the activation of the samples. The band at 1446 cm^{-1} is only observed in the Cu-modified zeolite. This band is attributed to the bending vibration δ(NH) of the NH groups [35], indicating that this zeolite sample is partially in the NH_4^+ form before activation, as a consequence of the ion-exchange pre-treatment with ammonia. After activation, NH_4^+ are removed and NZ-Cu presents free acidic hydroxyl groups.

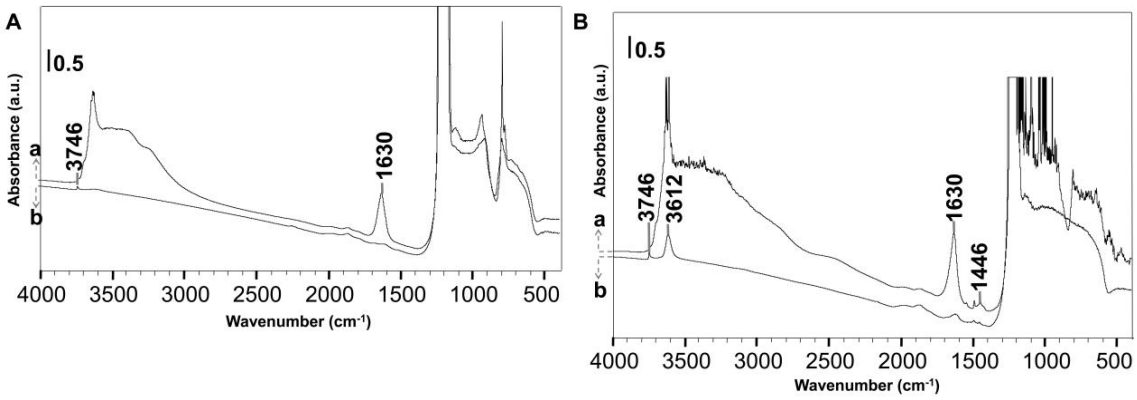

Fig. 2. Infrared spectra of zeolite samples: (A) natural zeolite, NZ, (B) Cu-modified zeolite, NZ-Cu. (a) before activation, (b) after activation.

Two IR bands are observed after the activation procedure at 3746 cm^{-1} and 3612 cm^{-1}. These bands are attributed to the vibration of silanol groups (Si-OH) and to the vibration of bridge hydroxyl groups (Si-OH-Al), respectively [36]. The latter band (3612 cm^{-1}) is generated after the ion-exchange step pre-treatment of natural zeolite, creating Brønsted acidity. It is worth noting that no band are visible between 3660 cm^{-1} and 3680 cm^{-1}, indicating that there is very little or no extra-framework aluminic OH phases formation during the activation of zeolite samples [32]. It is known that depending on the applied zeolite activation method (elimination of water), it can provoke partial dealumination of zeolite with the appearance of extra-framework aluminium (EFAL) species. The latter are usually detected upon pyridine adsorption, showing characteristic IR bands between 3660 and 3680 cm^{-1} [37, 38]. In this work, experimental evidences indicate that under the carried out activation procedure under secondary vacuum a dealumination process is quite unlikely to take place.

Fig. 3-A and 3-B depict IR bands evolution during pyridine dosing at 150°C on NZ and NZ-Cu, respectively. Curves (a) and (f) indicate the smaller and the higher applied doses of pyridine, respectively. Inserted graphs represent IR difference spectra between pyridine-adsorbed and activated (pyridine-free) samples. As it can be seen, the band at 3612 cm^{-1} decreases as a consequence of pyridine interaction with OH acidic groups. Nevertheless, this

band does not disappear completely, even after introduction of relatively high amounts of pyridine. This could be due to some of the acidic sites not being accessible to pyridine.

As indicated before, NZ is composed mainly of clinoptinolite (53%) and mordenite (40%). In the case of the porous framework of mordenite, it is formed by two types of elliptical channels. One of them is a 12-membered oxygen ring channel (6.7 x 7.8 A) and the other one is an 8-membered oxygen ring channel (2.9 x 5.7 A) often called “side pockets” [39-41] and usually not accessible to pyridine molecules. The overall amount of OH groups accessible to pyridine molecules in our samples remains low (lower than 4%) (see Table 2). It is possible that after Cu^{2+} ions incorporation, the opening windows of the 12-membered oxygen ring channel of the mordenite part of natural zeolite are partially blocked. IR bands at 1545, 1492 and 1454 cm^{-1} increase due to pyridine interaction with accessible Brønsted (B), Lewis and Brønsted (B+L) and Lewis (L) acid sites of zeolites, respectively.

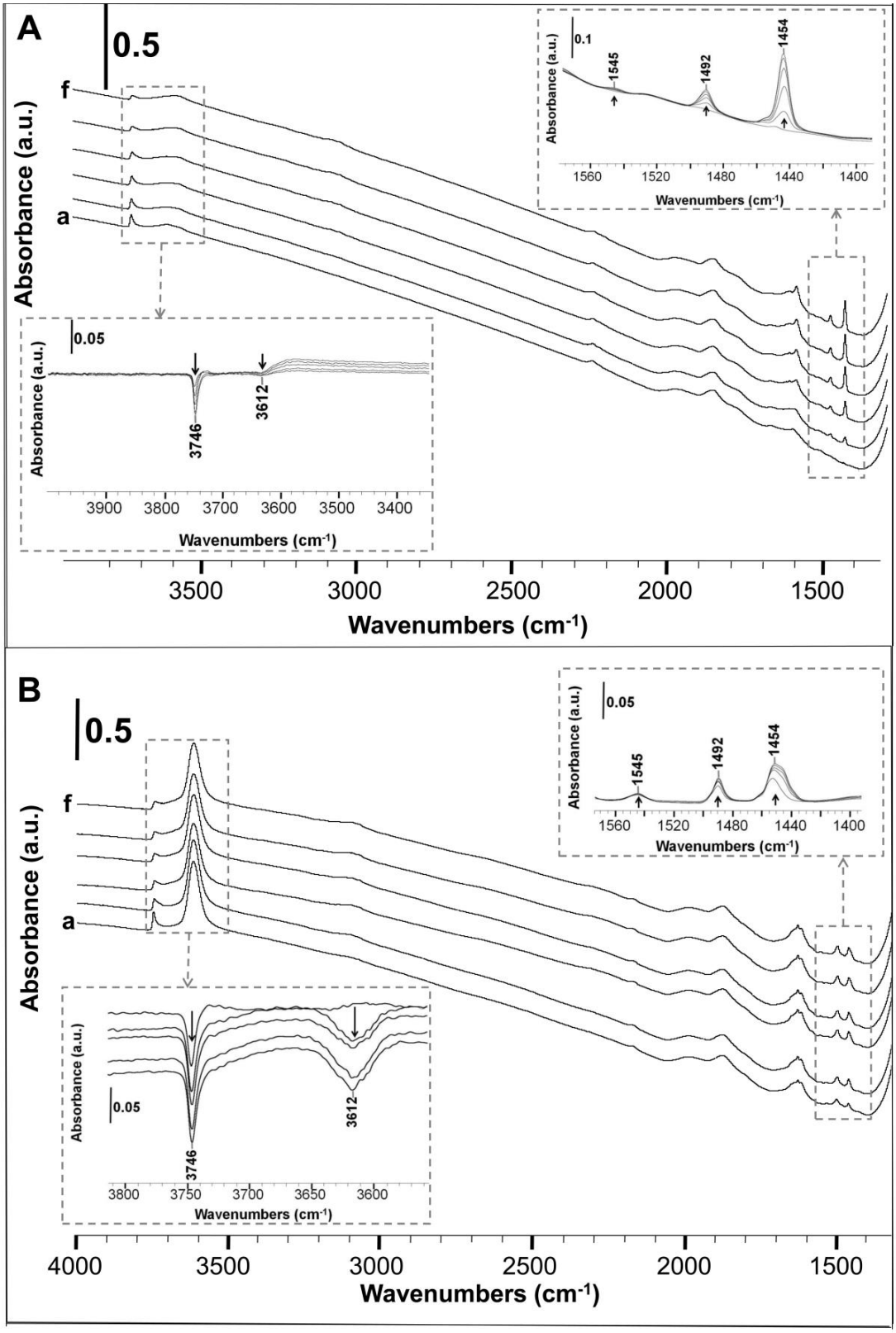
A
0.5
f
a
Absorbance (a.u.)
0.1
1545
1492
1454
1560
1520
1480
1440
1400
Wavenumbers (cm-1)
0.05
3746
3612
3900
3800
3700
3600
3500
3400
3500
3000
2500
2000
1500
Wavenumbers (cm-1)
B
0.5
f
a
Absorbance (a.u.)
0.05
1545
1492
1454
1560
1520
1480
1440
1400
Wavenumbers (cm-1)
0.05
3746
3612
3800
3750
3700
3650
3600
4000
3500
3000
2500
2000
1500
Wavenumbers (cm-1)

1

2

Fig. 3. Evolution of infrared bands of zeolite samples during pyridine dosing process at 150°C**:** (A) natural zeolite, NZ, (B) Cu-modified zeolite. Inserted graphs represent IR difference spectra between pyridine-adsorbed samples and unloaded samples (without pyridine). Curves (a) and (f) represent the smaller and the higher applied doses of pyridine, respectively.

Fig. 4-A and 4-B illustrate the IR bands evolution during pyridine desorption from natural and Cu-modified zeolite as temperature increases in the range 200 to 350°C, respectively. As it can be seen, natural zeolite presents a relatively high amount of Lewis acidic sites, probably due to the presence of Al^{3+} in the zeolite framework as a consequence of the low Si/Al molar ratio of this zeolite (Si/Al = 5.4). In the case of Cu-modified zeolite, during the ion-exchange pre-treatment step using ammonia, compensating cations balancing the zeolite framework negative charge are replaced by NH_4^+ ions which will give place to bridged hydroxyl groups generation after the out-gassing procedure at 350°C, creating thus Brønsted acidity. After Cu^{2+} ions incorporation into the zeolite sample, Lewis acidity is enhanced. However, it still remains lower compared to that of NZ. It is known that the temperature chosen for zeolite thermal treatments, the solution pH during the ion-exchange process, as well as the nature of the transition metal have a significant influence on the acidic character of zeolite samples [42]. The acidity presented in NZ-Cu could be explained by partial dealumination which causes zeolite dehydroxylation during the earlier thermal treatments applied to natural zeolite. The creation of several stacking faults in zeolite framework as well as the formation of copper clusters blocking the pores could explain the quite low accessibility of the OH groups of this sample. It is worth noticing that pyridine also interacts with isolated weakly acidic silanol groups (see the diminution of the IR band at 3746 cm^{-1}) as a consequence of the partial obstruction of more acidic OH groups in both samples.

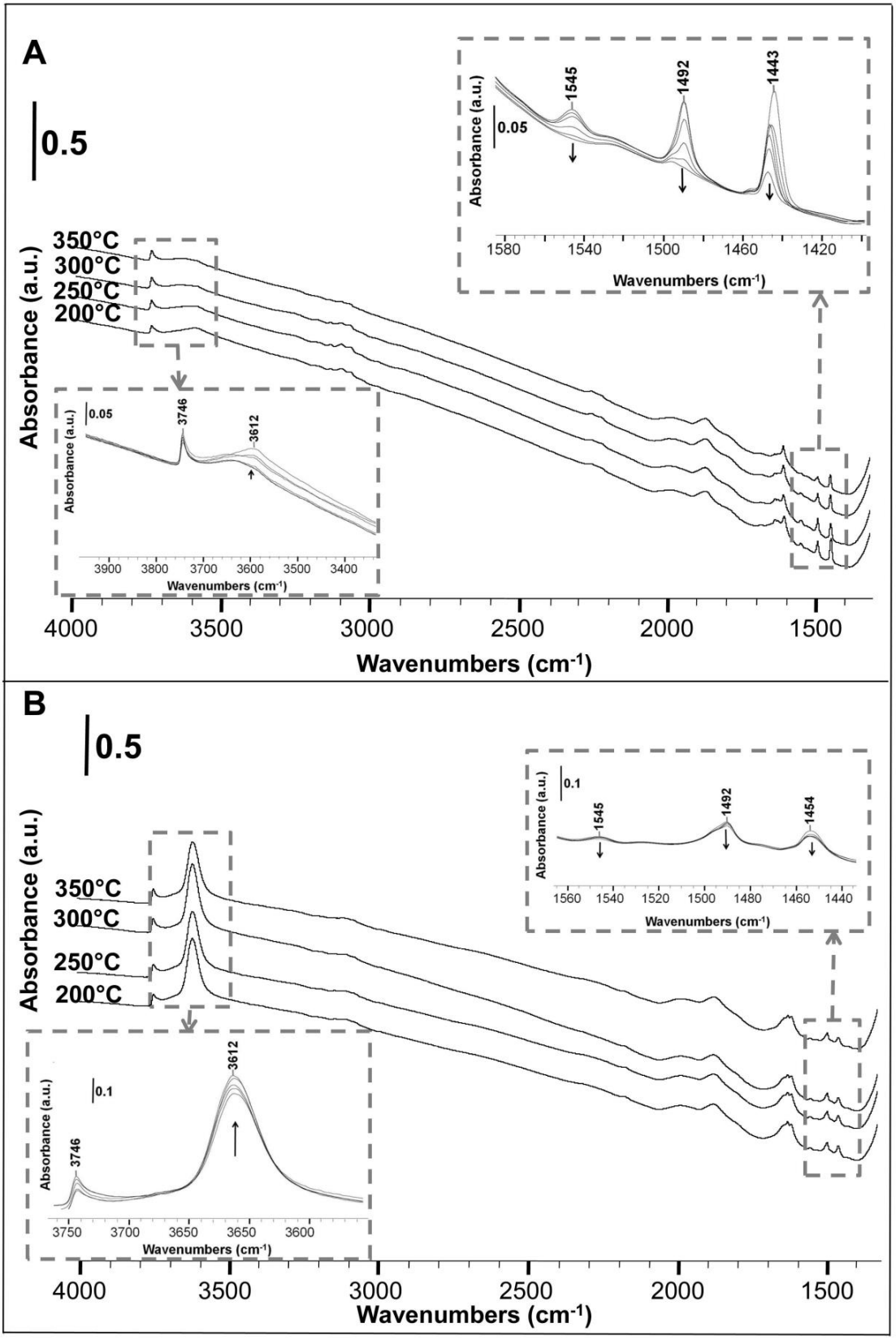
A
0.5
350°C
300°C
250°C
200°C
Absorbance (a.u.)
0.05
1545
1492
1443
1580
1540
1500
1460
1420
Wavenumbers (cm-1)
0.05
3746
3612
3900
3800
3700
3600
3500
3400
Wavenumbers (cm-1)
4000
3500
3000
2500
2000
1500
Wavenumbers (cm-1)
B
0.5
350°C
300°C
250°C
200°C
Absorbance (a.u.)
0.1
1545
1492
1454
1560
1540
1520
1500
1480
1460
1440
Wavenumbers (cm-1)
0.1
3612
3746
3750
3700
3650
3650
3600
Wavenumbers (cm-1)
4000
3500
3000
2500
2000
1500
Wavenumbers (cm-1)

1

Fig. 4. Evolution of infrared bands during pyridine desorption from zeolite samples at different temperatures. (A) natural zeolite, NZ, (B) Cu-modified zeolite.

Table 2. Lewis and Brønsted acidic site content (μmol g^{-1}) of natural (NZ) and Cu-modified zeolite (NZ-Cu), detected by quantifying the amount of pyridine retained after heating the samples from 200 to 350°C.

Sample	Heating Temperature (°C)	Lewis acid sites (μmol g^{-1})	Brønsted acid sites (μmol g^{-1})	Total acidity (μmol g^{-1})	Accessible OH groups
NZ	200	115.6	23.7	139.3	-
	250	80.5	25.4	105.9	
	300	69.6	17.9	87.5	
	350	60.3	9.9	70.2	
NZ-Cu	200	27.7	11.2	38.9	3.4%
	250	20.0	11.2	31.2	
	300	17.2	11.5	28.7	
	350	12.4	9.4	21.8	

Results listed in Table 2 reveal the presence of acidic surface sites of different strength. The amount of pyridine that remains adsorbed after heating zeolite samples from 200 to 350°C is related to the strength of Brønsted and Lewis acidic sites. Low (200–250ºC), mid (300°C) and high (350ºC) temperature ranges could be related to the desorption of pyridine from weak, middle and strong acidic sites, respectively. Thus, the strongest Brønsted and Lewis acidic sites are calculated as the amount of pyridine retained after heating the samples up to 350°C. On the one hand, the strength of Brønsted acidic sites is found to be enhanced after physicochemical transformation of natural zeolite (61.6% of pyridine remains adsorbed in NZ-Cu compared to 13.9% in NZ) and could be related to the sequence applied treatments of ammonium exchange, thermal out-gassing followed by post-calcination and hydrogen

reduction at 350°C; as well as to copper position within the zeolite framework. On the other hand, the strength of Lewis acidic sites in natural zeolite is not significantly modified after the applied chain of treatments conducted here (41.3% of pyridine remains adsorbed on NZ after out-gassing at 350°C compared to 47.7% for NZ-Cu).

The accessibility of deuterated acetonitrile (CD_3CN) to OH groups is presented in Table 3. As it can be noticed, OH groups of natural zeolite are not accessible, even using CD_3CN. However, the amount of accessible OH groups of Cu-modified zeolite using CD_3CN is higher than those when pyridine (C_5H_5N) is applied (see Table 1). CD_3CN is a basic probe with a smaller molecular size than C_5H_5N. Nonetheless, the OH groups' accessibility is still far away from 100%, confirming partial zeolite pore blockage.

Table 3. Accessible OH groups to deuterated acetonitrile (CD_3CN) of natural (NZ) and Cu-modified zeolite (NZ-Cu).

Sample	Accessible OH groups (%)
NZ	-
NZ-Cu	68.24

3.2. DRIFTS study of surface interactions among zeolite samples and target VOC_{Cl}

DRIFTS spectra of natural (NZ) and Cu-modified zeolite (NZ–Cu) during the adsorption of target VOC_{Cl} are depicted in Fig. 5 and 6, respectively. Fig. 5-A and 5-B show DRIFTS evolution during perchloroethylene and chlorobenzene adsorption onto NZ sample, respectively; while Fig. 6-A and 6-B show DRIFTS evolution during perchloroethylene and chlorobenzene adsorption onto NZ-Cu sample, respectively. It is worth noticing that the quality of Figures 5 and 6 are quite much lower than that of Figures 2 to 4, since Fig. 5 and 6 were obtained using DRIFTS under flow conditions and Fig. 2 to 4 were acquired under partial vacuum using IR transmission technique.

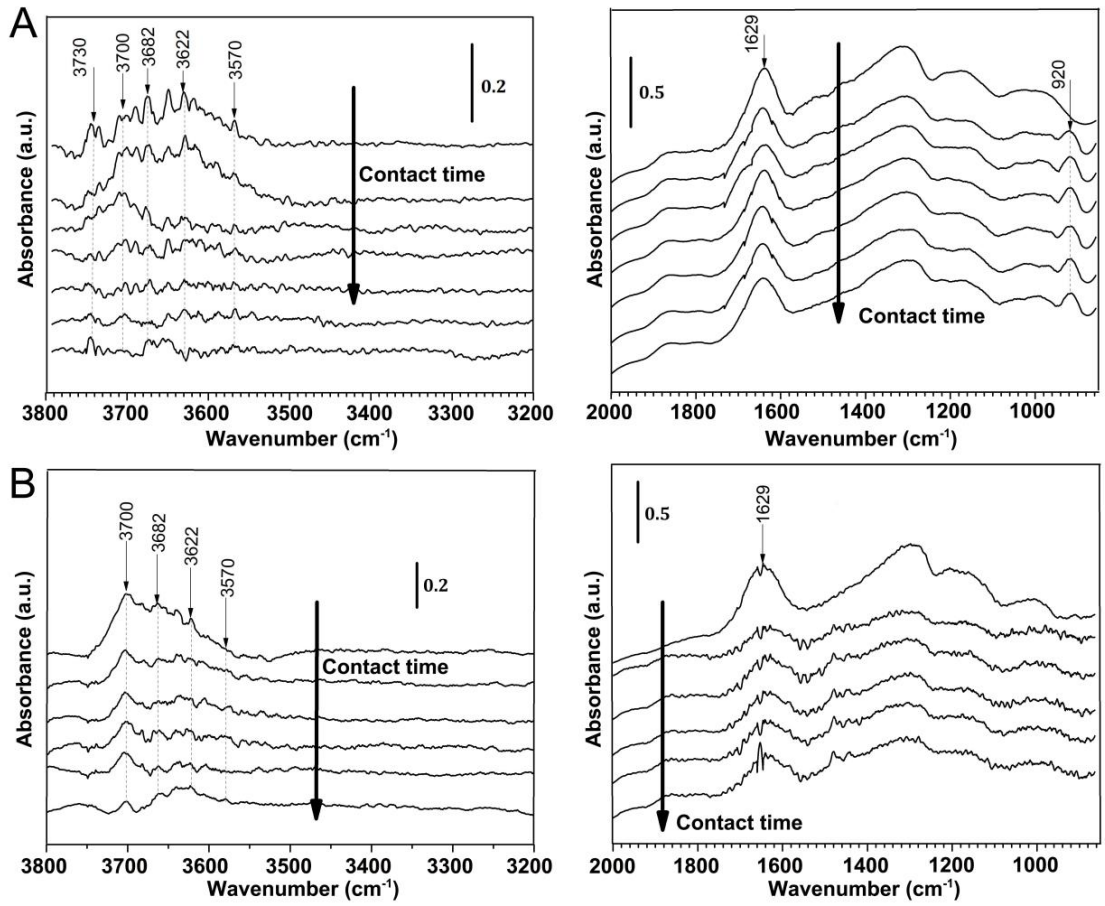

Fig. 5. Variation of DRIFTS spectra as a function of contact time during VOC_{Cl} adsorption onto NZ at 20°C: (A) perchloroethylene, (B) chlorobenzene. Operating conditions: 0.03 g of zeolite sample, 50 cm^3 min^{-1}, with an inlet concentration of perchloroethylene (or chlorobenzene) of 7.6 μmol dm^{-3}.

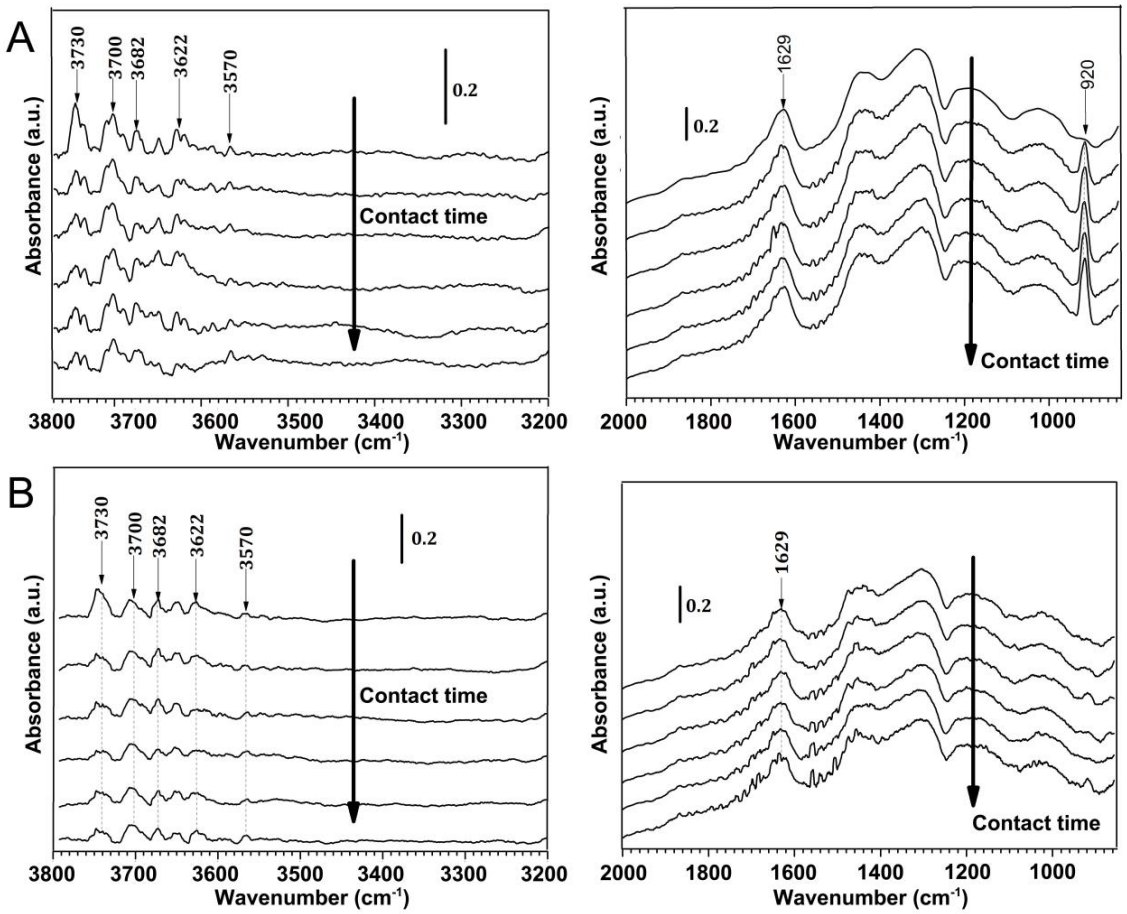

Fig. 6. Variation of DRIFTS spectra as a function of contact time during VOC_{Cl} adsorption onto NZ-Cu at 20°C: (A) perchloroethylene, (B) chlorobenzene. Operating conditions: 0.03 g of zeolite sample, 50 cm^3 min^{-1}, with an inlet concentration of perchloroethylene (or chlorobenzene) of 7.6 μmol dm^{-3}.

Infrared vibration bands at 3730 cm^{-1}, 3700 cm^{-1}, and 3570 cm^{-1} are probably perturbed after zeolite exposure to gaseous VOC_{Cl} (perchloroethylene and chlorobenzene) due to their interaction with zeolite active sites. The presence of new Lewis acid sites after Cu^{2+} incorporation into NZ lattice, are responsible for the observed enhancement of water adsorption. Therefore, new Brønsted acid sites are induced in Cu-modified zeolites upon water adsorption. In the presence of water, introduced copper over zeolite framework may first tend to coordinate water molecules that then through a dissociative chemisorption led to

the observed increase in the IR signal of OH groups. In both samples, the IR bands between 3730 and 3570 cm^{-1} are ascribed to OH groups of adsorbed water from carrier gas coming together with VOCs. An IR band located at 1629 cm^{-1} in both samples corresponds to flexion vibrations of the OH groups of residual water [36,43,44]. This band is closely related to IR bands from 3730 to 3570 cm^{-1}. Vibrational IR modes in the range between 1300 and 600 cm^{-1} correspond to zeolite lattice structure. These IR bands are caused by the stretching and bending modes of the T-O units. Double ring vibrations are found in the IR region between 650-600 cm^{-1} and between 1300-700 cm^{-1} related to O-T-O and T-O-T symmetric and antisymmetric stretching vibrations, respectively [45,46]. Such bands have little or no modification during the adsorption and desorption of the VOC_{Cl}.

In the spectrum of perchloroethylene adsorption (see Fig. 5-A and Fig. 6-A), a decrease in the intensity of the IR bands from 3730 to 3570 cm^{-1} is observed for both NZ and NZ-Cu. Additionally, a wide band around 1629 cm^{-1} is recorded in the low wavenumbers of the spectral range (see Fig. 5-A and Fig. 6-A). This band could be related to water reappearance coming in the carrier gas. In both samples, it is also observed an IR band increasing upon contact with perchloroethylene at 920 cm^{-1}. This band is assigned to perchloroethylene in gas phase after sample surface saturation. Perchloroethylene interacts, in both NZ and NZ-Cu samples, with their weakly acidic OH groups formed through water adsorption on zeolites. In the case of NZ-Cu, unlike NZ samples, the interaction of perchloroethylene with OH groups of adsorbed water is much higher because of the introduction of new Lewis acid sites (Cu^{2+}).

Similar behaviours to perchloroethylene interactions are observed in the case of chlorobenzene adsorption (see Fig. 5-B and Fig. 6-B). A decrease in the intensity of the IR bands from 3730 to 3570 cm^{-1} is also noticed in both zeolite samples. Analogous to perchloroethylene adsorption, in the case of chlorobenzene a band at 1629 cm^{-1} is also registered at lower wavenumbers (see Fig. 5-B and Fig. 6-B). This signal is also ascribed to

the reappearance of residual water coming in the carrier gas. In the case of NZ-Cu, in contrast to NZ samples, chlorobenzene interacts more strongly with new OH groups formed as a consequence of water adsorption over new Lewis acid sites generated by the insertion of copper. Additionally, the stretching vibrations of the aromatic ring of chlorobenzene molecule in the gas phase at 1589 and 1500 cm^{-1} (spectrum not shown here) [47,48] are recorded, indicating that both zeolite samples reach saturation by chlorobenzene.

3.3. Temperature-programmed desorption (TPD) of the adsorbed VOC_{Cl} onto zeolite samples

Fig. 7 displays the TPD profiles of the target VOC_{Cls} previously adsorbed on natural zeolite (NZ) and Cu-modified zeolite (NZ-Cu). Fig 7-A and Fig 7-B correspond to TPD profiles of perchloroethylene and chlorobenzene, respectively. In the case of perchloroethylene desorption from both zeolite samples, two overlapping peaks are observed. Lower temperature peaks reach a maximum around 109°C, being close to the boiling point of perchloroethylene (121°C). Such results could be related to the desorption of physisorbed perchloroethylene molecules. Second non-resolved peaks with a maximum desorption temperature around 200°C point out the presence of adsorption sites of higher strength. The evolution of perchloroethylene at 200°C from both zeolite samples could be related to perchloroethyelene interaction with strong acid sites. It is well known that the required energy to release a base probe molecule from acid sites is associated to the strength of the chemical bonds (acid strength) [33]. However, different results are exhibited for chlorobenzene evolution, where TPD profiles reveal two well-defined peaks in both samples. The first peaks with a maximum at 72°C could be related to the desorption of physisorbed chlorobenzene molecules, being congruent with its boiling point (131ºC). Second resolved peaks with a maximum around 300°C reflect how strongly some chlorobenzene molecules are bonded to active surface sites.

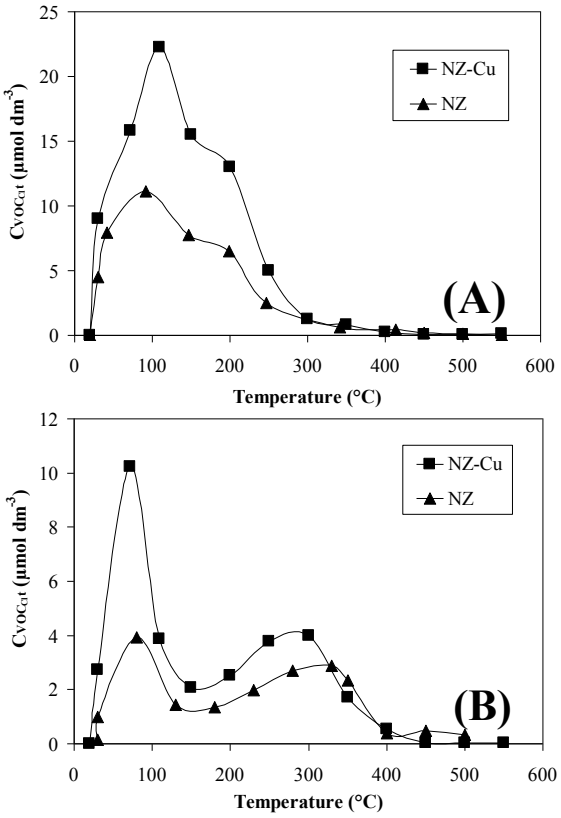

Fig. 7. Temperature-programmed desorption profiles of adsorbed VOC_{Cl}: (A) perchloroethylene, (B) chlorobenzene. (▲) after adsorption onto natural zeolite at 20°C. (■) after adsorption onto Cu-modified zeolite. Experimental conditions: Desorption under argon flow (100 cm^3 min^{-1}), heating up to 550°C at 3°C min^{-1}.

Table 4. Comparison of perchloroethylene and chlorobenzene adsorption and desorption on natural zeolite (NZ) and Cu-modified zeolite (NZ-Cu).

VOC_{Cls}	Q_a [a] (μmol g^{-1})		Q_d [b] (μmol g^{-1})	
	NZ	**NZ-Cu**	**NZ**	**NZ-Cu**
Perchloroethylene	68.5	177.9	63.8	131
Chlorobenzene	51.8	166.5	26.8	50.3

[a] Total amount of adsorbed VOC_{Cl} at 20°C.

[b] Total amount of desorbed VOC_{Cl} after heating the sample under Ar flow (100 cm^3 min^{-1}) up to 550 ºC at 3 ºC min^{-1}.

In addition, the amounts of thermally desorbed perchloroethylene and chlorobenzene are lower than the adsorbed amounts (see Table 4). These results not only reflect the influence of molecular size of the target VOC_{Cl} on the adsorption capacity but also corroborate the existence of chemical surface interactions between the VOC_{Cl} and the active surface sites of zeolite samples. In particular, the highest observed adsorption capacity of NZ-Cu towards perchloroethylene could be related to a higher migration of perchloroethylene molecules through the channels of this zeolite sample, reaching more available adsorption sites in the small cages, compared to NZ zeolite. Results listed in Table 4 show that perchloroethylene and chlorobenzene are thermally desorbed from NZ-Cu at 74% and 30%, respectively; whereas from NZ they are thermally evolved at 93% and 52%, respectively. The lowest desorbed amount of chlorobenzene molecules from NZ-Cu zeolite might be a consequence of strong chemical interactions between chlorobenzene molecules and Brønsted acid sites of this zeolite framework. Such results are in agreement with those obtained by DRIFTS analyses. These results suggest that chlorobenzene and perchloroethylene are bonded to different types of OH groups of NZ-Cu surface with varying adsorption strength distributions. A higher amount of evolved perchloroethylene at mid temperature could be related to the interaction with OH groups original present on the zeolite surface; whereas upper temperature evolution of chlorobenzene could be associated to strong interactions with OH groups formed after the applied modification treatments. Therefore, TPD results evidence the different adsorption strength of the formed electron pair donor-acceptor surface complex, as described in another publication [49].

3.4. Mechanistic approach

Perchloroethylene and chlorobenzene adsorption onto NZ and NZ-Cu could be represented by a mechanism that incorporates the interaction not only with Brønsted (Z-OH) sites present on the original natural zeolite framework; but also with new Brønsted acid sites, formed as a consequence of dissociative chemisorption of water molecules over new Lewis acid sites generated due to the insertion of copper after the successive treatments applied in this work (see Fig. 8).

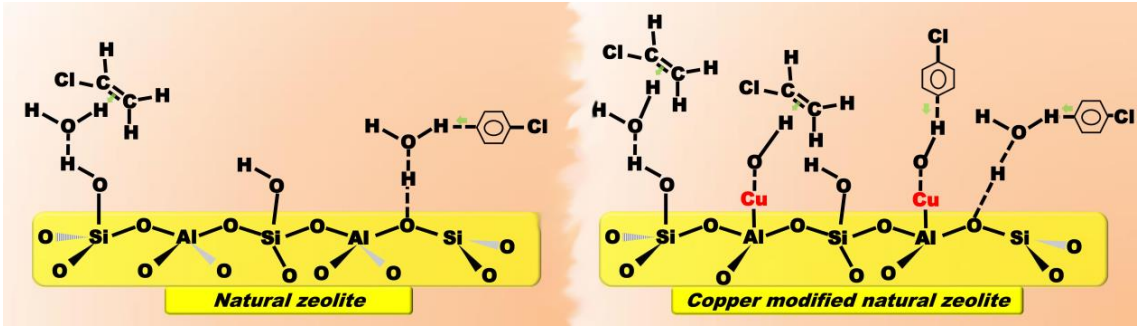

Fig. 8. Schematic representation of the interaction of perchloroethylene and chlorobenzene molecules with original and new Brønsted (Z-OH) sites formed as a consequence of dissociative chemisorption of water molecules over new Lewis acid sites.

Perchloroethylene and chlorobenzene molecules are able to have contact with Brønsted acid sites (Z-OH) of NZ and NZ-Cu surfaces, forming hydrogen bonding, according to Eq. (2):

$$\text{Z-OH} + \text{VOC}_{\text{Cl}} \leftrightarrow \text{Z-OH}\cdots\text{VOC}_{\text{Cl}} \quad (2)$$

The adsorption interaction of VOC_{Cls} with active surface sites of natural and Cu-modified zeolites is modelled using the Langmuir adsorption approach. The rate of adsorption-desorption of VOC_{Cl} at Brønsted acid sites (r^{Z-OH}, $m^2\ m^{-2}\ s^{-1}$) is represented by the following expression:

$$r^{Z-OH} = k_{ad}^{Z-OH} S_{VOC_{Cl}} N_A \{Z-OH\}_v C_{VOC_{Cl}} - k_{des}^{Z-OH} S_{VOC_{Cl}} N_A \{Z-OH\cdots VOC_{Cl}\} \quad (3)$$

where k_{ad}^{Z-OH} ($dm^3\ s^{-1}\ \mu mol^{-1}$) and k_{des}^{Z-OH} (s^{-1}) represent forward and reverse rate constants of VOC_{Cl} surface complex formation at Brønsted acid sites, respectively. $S_{VOC_{Cl}}$ (m^2 adsorbate molecule^{-1}) is the cross-sectional area of the target VOC_{Cl} molecule, and N_A is the Avogadro constant (6.022×10^{23} molecules mol of adsorbate^{-1}). $\{Z\text{-}OH\}_v$ (mol m^{-2}) represents the total vacant Brønsted acid sites or the total surface concentration of Brønsted acid sites. $\{Z\text{-}OH\cdots VOC_{Cl}\}$ (mol m^{-2}) is the amount of VOC_{Cl} adsorbed at Brønsted acid sites. $C_{VOC_{Cl}}$ ($\mu mol\ dm^{-3}$) is the concentration of the target VOC_{Cl}. An analogous adsorption mechanism has been suggested to represent the adsorption of VOCs onto acidic zeolites [28,50].

When the equilibrium is reached, the rates of adsorption and desorption are the same and the adsorption equilibrium constant is described, according to Eq. (4):

$$K_{eq} = \frac{k_{ad}^{Z-OH}}{k_{des}^{Z-OH}} = \frac{\{Z-OH\cdots VOC_{Cl}\}}{\{Z-OH\}_v C_{VOC_{Cl}}} \quad (4)$$

where K_{eq} ($dm^3\ \mu mol^{-1}$) is the adsorption equilibrium constant of the VOC_{Cl} surface complex formation at Brønsted acid sites.

A site balance is used to eliminate the unknown acidic surface site concentration, $\{Z\text{-}OH\}_v$. Thus, the total concentration of Brønsted acid sites, Z_t (mol m^{-2}), is given by Eq. (5):

$$Z_t = \{Z-OH\}_v + \{Z-OH\cdots VOC_{Cl}\} \quad (5)$$

Replacing Eq. (5) into Eq. (3) results in Eq. (6), which is the usual form of the Langmuir equation:

$$\theta^{Z-OH\cdots VOC_{Cl}} = \frac{K_{eq} C_{VOC_{Cl}} Z_t S_{VOC_{Cl}} N_A}{1 + K_{eq} C_{VOC_{Cl}}} \quad (6)$$

where $\theta^{Z-OH\cdots VOC_{Cl}}$ ($m^2\ m^{-2}$) stands for the fraction of the covered OH groups of both zeolite samples (NZ or NZ-Cu) with the target VOC_{Cl} molecule (perchloroethylene or chlorobenzene) at equilibrium, Z_t (mol m^{-2}) is the maximum adsorption capacity toward the target VOC_{Cl}, corresponding to monolayer coverage (NZ or NZ-Cu) or zeolite saturation,

$C_{VOC_{Cl}}$ (μmol dm^{-3}) is the concentration of the target VOC_{Cl} (perchloroethylene or chlorobenzene) at the equilibrium, $S_{VOC_{Cl}}$ (m^2 adsorbate molecule^{-1}) is the cross-sectional area of the target VOC_{Cl} molecule, and N_A is the Avogadro constant (6.022 ×10^{23} molecules mol of adsorbate^{-1}).

Fig. 9-A and Fig 9-B display adsorption equilibrium data obtained at 20 ºC of perchloroethylene and chlorobenzene onto zeolite samples (NZ and NZ-Cu), respectively. Table 5 lists the equilibrium parameters of the Langmuir model, such as: the maximum adsorption capacity, Z_t, and the adsorption equilibrium constant, K_{eq}, together with the correlation factor R^2. Adsorption data are well-adjusted to the Langmuir model.

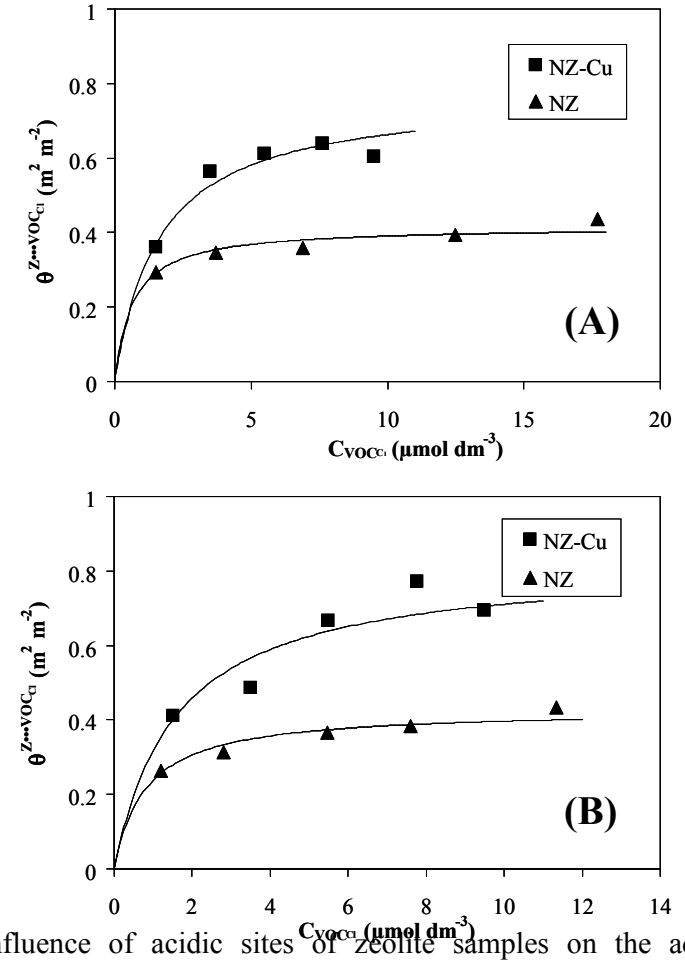

Fig. 9. Influence of acidic sites of zeolite samples on the adsorption of VOC_{Cl}: (A) perchloroethylene, (B) chlorobenzene. (▲) natural zeolite, NZ; (■) Cu-modified zeolite, NZ-

Cu. Thin lines represent the fits to the Langmuir adsorption model. Experimental conditions: 0.3 g of zeolite, 50 cm^3 min^{-1}, 101 kPa, 20°C.

Table 5.

Comparison of Langmuir adsorption equilibrium constants of perchloroethylene and chlorobenzene onto natural (NZ) and Cu-modified zeolite (NZ-Cu) at 20ºC.

Sample	VOC_{Cl}	Z_t ($\mu mol\ g^{-1}$)	Z_t ($m^2\ m^{-2}$)	K_{eq} ($dm^3\ \mu mol^{-1}$)	R^2
NZ	Perchloroethylene	93	0.42	1.52	0.89
	Chlorobenzene	71	0.43	1.25	0.94
NZ-Cu	Perchloroethylene	222	0.77	0.61	0.96
	Chlorobenzene	179	0.82	0.63	0.87

As it can be seen in Table 5, the values of maximum adsorption capacities (Z_t) of Cu-modified zeolite toward both target VOC_{Cls} are increased after the successive chemical and thermal treatments applied to the natural zeolite. These results agree with those previously reported for the adsorption of different kind of VOCs onto synthetic mordenite zeolites, natural and acid-treated natural mordenite [28,51-53]. The highest adsorption capacity obtained by NZ-Cu zeolite could be due to a combination of physical and chemical factors. As discussed before, the physicochemical transformation of NZ into NZ-Cu, produces a zeolite with a higher specific surface area, pore volume and with a similar strength of Lewis acidic sites but with stronger Brønsted acidic sites. The small cross-sectional area of perchloroethylene molecules (0.18 nm^2) as compared to chlorobenzene molecules (0.24 nm^2) might allow easier access for perchloroethylene molecules to acidic sites in the small pores of both zeolite samples. In the case of NZ, narrow pores impose higher spatial constraints,

reducing the adsorption capacity of this sample toward perchloroethylene and chlorobenzene molecules. Indeed, results suggest that NZ might inhibit the access of chlorobenzene molecules to acidic surface sites, leading to a reduction on the observed adsorption capacity of this zeolite sample. In the case of NZ-Cu zeolite the adsorption capacity is less affected. Chlorobenzene molecules could migrate inside this zeolite framework, having a dual-site interaction at acidic hydroxyl sites such as Si(OH)Al and silanol groups original present in natural zeolite and also at OH groups formed over Lewis acid sites like Cu^{+} cations due to dissociative chemisorption of water in modified natural zeolite surface, forming adsorption complexes [49].

4. Conclusions

Results indicated that a succession of ion-exchange with ammonium salt, thermal out-gassing at 350°C, and ion-exchange using Cu^{2+} salt (0.05 mol dm^{-3}) followed by calcination and reduction under hydrogen at 350°C produced a Cu-modified zeolite with increased adsorption capacity for the elimination of VOC_{Cl} compared to the natural zeolite. DRIFTS assays revealed that the modified zeolite contains mainly a single class of active site for the adsorption of VOC_{Cl}. DRIFTS spectra indicated that the modified NZ-Cu zeolite exhibits an enhanced acidic character due to the presence of Brønsted acid sites present on the original natural zeolite framework together with new Brønsted acid sites formed after the applied modification treatments. In the presence of water, water was adsorbed on new Lewis acid sites generated after copper incorporation into the zeolite structure, leading to the formation of new Brønsted acid sites through a dissociative chemisorption. Hence, Brønsted acid sites play a fundamental role in the adsorption mechanism of VOC_{Cl}. Assessed targets VOC_{Cl} interacted with Brønsted acid sites, forming hydrogen bonds. A combination of chemical and thermal

treatment results in a powerful procedure to improve the adsorption capacity of natural zeolitic materials as potential adsorbents for the removal of VOC_{Cl} from contaminated industrial streams.

Acknowledgements

This research was financially support by CONICYT, FONDECYT/Regular (Grant No. 1130560). A.L. Riquelme thanks the *Programa de Magíster en Ingeniería Industrial* from the *Universidad Católica de la Santísima Concepción* for providing a Master research fellowship.

References

[1] Q. Huang, Z. Meng, R. Zhou, The effect of synergy between Cr_2O_3-CeO_2 and USY zeolite on the catalytic performance and durability of chromium and cerium modified USY catalysts for decomposition of chlorinated volatile organic compounds, Appl. Catal. B-Environ. 115–116 (2012) 179–189. https://doi.org/10.1016/j.apcatb.2011.12.028

[2] V-H. Vu, J. Belkouch, A. Ould-Dris, B. Taouk, Removal of hazardous chlorinated VOCs over Mn–Cu mixed oxide based catalyst, J. Hazard. Mater. 169 (2009) 758–765. https://doi.org/10.1016/j.jhazmat.2009.04.010

[3] J. Lemus, M. Martin-Martinez, J. Palomar, L. Gomez-Sainero, M. Gilarranz, J. Rodriguez, Removal of chlorinated organic volatile compounds by gas phase adsorption with activated carbon, Chem. Eng. J. 211–212 (2012) 246–254. https://doi.org/10.1016/j.cej.2012.09.021

[4] H. Sidebottom, J. Franklin, The atmospheric fate and impact of hydrochlorofluorocarbons and chlorinated solvents, Pure Appl. Chem. 68 (1996) 1757–1769. https://doi.org/10.1351/pac199668091757

[5] S. H. Hsua , C. S. Huanga , T. W. Chunga, S. Gao, Adsorption of chlorinated volatile organic compounds using activated carbon made from *Jatropha* curcas seeds, J. Taiwan Inst. Chem. E. 45 (2014) 2526–2530. https://doi.org/10.1016/j.jtice.2014.05.028

[6] R. Iranpour, H. Coxa, M. Deshusses, E. Schroeder, Literature review of air pollution control biofilters and biotrickling filters for odor and volatile organic compound removal, Environ. Prog. 24 (2005) 254–267. https://doi.org/10.1002/ep.10077

[7] USEPA, EPA's Terms of Environment Glossary, Abbreviations, and Acronyms. Code of Federal Regulations, 40: Chapter 1, Subchapter C, Part 51, Subpart F, 51100, Retrieved on 2009–02–08.

[8] B. Huang, Ch. Lei, Ch. Wei, G. Zeng, Chlorinated volatile organic compounds (Cl-VOCs) in environment sources, potential human health impacts, and current remediation technologies, Environ. Int. 71 (2014) 118–138. https://doi.org/10.1016/j.envint.2014.06.013

[9] F.I. Khan, A.K. Ghoshal, Removal of volatile organic compounds from polluted air, J. Loss Prevent. Proc. 13 (2000) 527–545. https://doi.org/10.1016/S0950-4230(00)00007-3

[10] A.K. Ghoshal, S.D. Manjare, Selection of appropriate adsorption technique for recovery of VOCs: an analysis, J. Loss Prevent. Proc. 15 (2002) 413–421. https://doi.org/10.1016/S0950-4230(02)00042-6

[11] K. van Craeynest, H. van Langenhove, R.M. Stuetz, AOPs for VOCs and odour treatment, in: Simon Parsons (Ed.), Advanced Oxidation Processes for Water and Wastewater Treatment, IWA Publishing, 2004. Chapter 11.

[12] M. Guillemot, J. Mijoin, S. Mignard, P. Magnoux, Adsorption of perchloroethylene (PCE) in gas phase on zeolites of faujasite type: Influence of water vapour and of Si/Al ratio, Micropor. Mesopor. Mater. 111 (2008) 334–342. https://doi.org/10.1016/j.micromeso.2007.08.035

[13] C. Mouvet, D. Barberis, A.C.M. Bourg, Adsorption isotherms of tri- and perchloroethylene by various natural solids, J. Hydrol. 149 (1993) 163–182. https://doi.org/10.1016/0022-1694(93)90105-I

[14] A.H. Englert, J. Rubio, Characterization and environmental application of a Chilean natural zeolite, Int. J. Miner. Process 75 (2005) 21–29. https://doi.org/10.1016/j.minpro.2004.01.003

[15] S.W. Baek, J.R. Kim, S.K. Ihm, Design of dual functional adsorbent/catalyst system for the control of VOC's by using metal-loaded hydrophobic Y-zeolites, Catal. Today 93–95 (2004) 575–581. https://doi.org/10.1016/j.cattod.2004.06.107

[16] R. López-Fonseca, B. de Rivas, J.I. Gutiérrez-Ortiz, A. Aranzabal, J.R. González-Velasco, Enhanced activity of zeolites by chemical dealumination for chlorinated VOC abatement, Appl. Catal. B-Environ. 41 (2003) 31–42. https://doi.org/10.1016/S0926-3373(02)00199-6

[17] P. S. Chintawar, H. L. Greene, Adsorption and catalytic destruction of trichloroethylene in hydrophobic zeolites, Appl. Catal. B-Environ. 14 (1-2) (1997) 37–47. https://doi.org/10.1016/S0926-3373(97)00010-6

[18] B. Clausse, B. Garrot, C. Cornier, C. Paulin, M-H. Simonot-Grange, F. Boutros, Adsorption of chlorinated volatile organic compounds on hydrophobic faujasite: correlation between the thermodynamic and kinetic properties and the prediction of air cleaning, Micropor. Mesopor. Mater. 25 (1998) 169–177. https://doi.org/10.1016/S1387-1811(98)00202-9

[19] M. Hosseini; M. Haghighi; D. Kahforoushan; M. Zarrabi, Sono-dispersion of ceria and palladium in preparation and characterization of Pd/Al_2O_3-clinoptilolite-CeO_2 nanocatalyst for treatment of polluted air via low temperature VOC oxidation, Process Saf. Environ. 106 (2017) 284–293. https://doi.org/10.1016/j.psep.2016.06.028

[20] A.Z. Abdullah, M.Z.A. Bakar, S. Bhatia, Performance of H-ZSM-5-supported bimetallic catalysts for the combustion of polluting volatile organic compounds in air, J. Chem. Technol. Biot. 80 (2005) 1016–1025. https://doi.org/10.1002/jctb.1278

[21] M. Guillemot, J. Mijoin, S. Mignard, P. Magnoux, Volatile organic compounds (VOCs) removal over dual functional adsorbent/catalyst system, Appl. Catal. B-Environ. 75 (2007) 249–255. https://doi.org/10.1016/j.apcatb.2007.04.020

[22] G. Pozan, Z. Ozcelik , I. Boz, Total oxidation of toluene over metal oxides supported on a natural clinoptilolite-type zeolite, Chem. Eng. J., 162 (2010) 380–387. https://doi.org/10.1016/j.cej.2010.05.020

[23] Z. Özçelik, G.S.P Soylu, I. Boz, Catalytic combustion of toluene over Mn, Fe and Co-exchanged clinoptilonite support, Chem. Eng. J. 155 (2009) 94–100. https://doi.org/10.1016/j.cej.2009.07.013

[24] L.Yosefi, M. Haghighi, S. Allahyari, R. Shokrani, S. Ashkriz, Abatement of toluene from polluted air over Mn/Clinoptilolite–CeO_2 nanopowder: Impregnation vs. ultrasound assisted synthesis with various Mn-loading. Adv. Powder Tech. 26 (2015) 602–611. https://doi.org/10.1016/j.apt.2015.01.009

[25] Z. Jamalzadeh, M. Haghighi, N. Asgari, Synthesis and physicochemical characterizations of nanostructured Pd/carbon-clinoptilolite-CeO_2 catalyst for abatement of xylene from waste gas streams at low temperature, Ind. Eng. Chem. J. 20 (2014) 2735–2744. https://doi.org/10.1016/j.jiec.2013.11.001

[26] A. Riquelme, H. Valdés. Application of D-optimal design for modelling the adsorption of Cl-VOCs onto modified natural zeolites, Ingeniare 24 (2016) 542-557. http://dx.doi.org/10.4067/S0718-33052016000400002

[27] N.J. Abreu, H. Valdés, C.A. Zaror, F. Azzolina-Jury, M. Meléndrez, Ethylene adsorption onto natural and metal modified Chilean zeolite: an *Operando* DRIFTS

approach, Micropor. Mesopor. Mater. 274 (2019) 138–148. https://doi.org/10.1016/j.micromeso.2018.07.043

[28] H. Valdés, V. A. Solar, E. H. Cabrera, A. F. Veloso, C. A. Zaror. Control of released volatile organic compounds from industrial facilities using natural and acid-treated mordenites: The role of acidic surface sites on the adsorption mechanism. Chem. Eng. J. 244 (2014) 117–127. https://doi.org/10.1016/j.cej.2014.01.044

[29] S. Alejandro, H. Valdés, M.-H. Manero, C.A. Zaror, BTX abatement using natural zeolite: the role of Brønsted acid sites. Water Sci. Technol. 66 (2012) 1759-1765. https://doi: 10.2166/wst.2012.390

[30] S. Alejandro, H. Valdés, M.-H. Manero, C.A. Zaror, Oxidative regeneration of toluene-saturated natural zeolite by gaseous ozone: the influence of zeolite chemical surface characteristics, J. Hazard. Mater. 274 (2014) 212-220. http://dx.doi.org/10.1016/j.jhazmat.2014.04.006

[31] C.A. Emeis. Determination of integrated molar extinction coefficients for infrared absorption bands of pyridine adsorbed on solid acid catalysts. J. Catal. 141 (1993) 347–354. https://doi.org/10.1006/jcat.1993.1145

[32] S. Bordiga, C. Lamberti, F. Bonino, A. Travert, F. Thibault-Starzyk, Probing zeolites by vibrational spectroscopies, Chem. Soc. Rev. 44 (2015) 7262. https://doi.org/10.1039/C5CS00396B

[33] H. Valdés, S. Alejandro, C.A. Zaror, Natural zeolite reactivity towards ozone: The role of compensating cations, J. Hazard. Mater. 227-228 (2012) 34-40. https://doi.org/10.1016/j.jhazmat.2012.04.067

[34] F. Azzolina-Jury, F. Thibault-Starzyk, Mechanism of low pressure plasma-assisted CO_2 hydrogenation over Ni-USY by microsecond time-resolved FTIR spectroscopy, Top. Catal. 60 (2017) 1709-1721. https://doi.org/10.1007/s11244-017-0849-2

[35] D. Perra, N. Drenchev, K. Chakarova, M.G. Cutrufello, K. Hadjiivanov, Remarkable acid strength of ammonium ions in zeolites: FTIR study of low-temperature CO adsorption on NH_4FER, RSC Adv. 4 (2014) 56183. DOI: 10.1039/c4ra12504e

[36] F. Thibault-Startzyk, F. Maugé, Infrared spectroscopy. In: M. Che, J. Védrine (eds) Characterization of solid materials and heterogeneous catalysts: from structure to surface reactivity, pp 3–48. Wiley, New Jersey.

[37] F. Benaliouche, Y. Boucheffa, P. Ayrault, S. Mignard, P. Magnoux, NH3-TPD and FTIR spectroscopy of pyridine adsorption studies for characterization of Ag- and Cu-exchanged X zeolites, Micropor. Mesopor. Mater. 111 (2008) 80–88. https://doi.org/10.1016/j.micromeso.2007.07.006

[38] J.L. Agudelo ,E.J.M.Hensen, S.A.Giraldo, L.J.Hoyos, Influence of steam-calcination and acid leaching treatment on the VGO hydrocracking performance of faujasite zeolite, Fuel Process. Technol.133 (2015) 89–96. http://dx.doi.org/10.1016/j.fuproc.2015.01.011

[39] M. Król, W. Mozgawa, W. Jastrzebski, Theoretical and experimental study of ion-exchange process on zeolites from 5-1 structural group, J. Porous Mater. 23 (2016) 1–9. https://doi.org/10.1007/s10934-015-0050-6

[40] R. Gounder, E. Iglesia, Effects of partial confinement on the specificity of monomolecular alkane reactions for acid sites in side pockets of mordenite, Angew. Chem. Int. Ed. 49 (2010) 808–811. https://doi.org/10.1002/anie.200905869

[41] N.S. Nesterenko, F. Thibault-Starzyk, V. Montouillout, V.V. Yuschenko, C. Fernandez, J.-P. Gilson, F. Fajula, I.I. Ivanova, Accessibility of the acid sites in dealuminated small-port mordenites studied by FTIR of co-adsorbed alkyl pyridines and CO, Micropor. Mesopor. Mat. 71 (2004) 157–166. https://doi.org/10.1016/j.micromeso.2004.03.028

[42] F. Azzolina-Jury, I. Polaert, L.Estel, L.B. Pierella, Synthesis and characterization of MEL and FAU zeolites doped with transition metals for their application to the fine

chemistry under microwave irradiation, Appl. Catal. A-Gen. 453 (2013) 92–101. https://doi.org/10.1016/j.apcata.2012.11.046

[43] L. Mariey, J. Lamotte, T. Chevreau, J.C. Lavalley, FT-IR study of coked HY zeolite regeneration using oxygen or ozone, React. Kinet. Catal. Lett. 59 (1996) 241–246. https://doi.org/10.1007/BF02068119

[44] K. Byrappa, B.V.S. Kumar, Characterization of zeolites by infrared spectroscopy, Asian J. Chem. 19 (2007) 4933-4935. http://www.asianjournalofchemistry.co.in/User/ViewFreeArticle.aspx?ArticleID=19_6_118

[45] A. Jentys; J. A. Lercher, Techniques of zeolite characterization, in: H. van Bekkum; P.A. Jacobs; E.M. Flanigen, J.C. Jansen (Eds.), *Introduction to Zeolite Science and Practice*, Stud. Surf. Sci. Catal. 137 (2001) 345–386.

[46] A. Ballandras, G. Weber, C. Paulin, J.-P. Bellat, M. Rotger, Communication: Evidence of structural phase transitions in silicalite-1 by infrared spectroscopy, J. Chem. Phys. 139 (2013) 091103–091104. https://doi.org/10.1063/1.4819080

[47] M. Govindarajan, M. Karabacak, V. Udayakumar, S. Periandy, FT-IR, FT-Raman and UV spectral investigation: Computed frequency estimation analysis and electronic structure calculations on chlorobenzene using HF and DFT, Spectrochim. Acta, Part A 88 (2012) 37– 48. https://doi.org/10.1016/j.saa.2011.11.052

[48] M. Reichenbächer, J. Popp, Challenges in Molecular Structure Determination. Springer-Verlag, Berlin Heidelberg, 2012.

[49] J.A. Lercher, C. Gründling, G. Eder-Mirth, Infrared studies of the surface acidity of oxides and zeolites using adsorbed probe molecules, Catal. Today 27 (1996) 353–376. https://doi.org/10.1016/0920-5861(95)00248-0

[50] H. Knozinger, S. Huber, IR spectroscopy of small and weakly interacting molecular probes for acidic and basic zeolites, J. Chem. Soc., Faraday Trans. 94 (1998) 2047–2059. https://doi.org/10.1039/A802189I

[51] S.-I. Kim, T. Aida, H. Niiyama, Binary adsorption of very low concentration ethylene and water vapor on mordenites and desorption by microwave heating, Separ. Purif. Technol. 45 (2005) 174–182. https://doi.org/10.1016/j.seppur.2005.03.006

[52] R. Arletti, A. Martucci, A. Alberti, L. Pasti, M. Nassi, R. Bagatin, Location of MTBE and toluene in the channel system of the zeolite mordenite: Adsorption and host–guest interactions, J. Solid State Chem. 194 (2012) 135–142. https://doi.org/10.1016/j.jssc.2012.04.024

[53] A. Martucci, L. Pasti, M. Nassi, A. Alberti, R. Arletti, R. Bagatin, R. Vignola, R. Sticca, Adsorption mechanism of 1,2-dichloroethane into an organophilic zeolite mordenite: A combined diffractometric and gas chromatographic study, Micropor. Mesopor. Mater. 151 (2012) 358–367. https://doi.org/10.1016/j.micromeso.2011.10.010